Batch-Sequential Maximum One-Factor-At-A-Time Designs

Qian Xiao

Shanghai Jiao Tong University

Joint research with Qiang Zhao, Chunwei Zheng, Fasheng Sun

Outline

Outline

Introduction

Factor screening (variable selection or sensitivity analysis)

- Classic OFAT, FFD, DSD under linear models.
- Highly nonlinear and computationally expensive computer models.
- Model-free vs model specific approaches.

Two popular model-free approach

- Morris screening (Morris 1991).
- Sobol' method (Sobol' 1990, 1993).

Morris Screening

- Morris (1991) defined elementary effects via OFAT:

$$d_i(\mathbf{x}) = \frac{y(\mathbf{x}_i(\Delta)) - y(\mathbf{x})}{\Delta}, \quad i = 1, \dots, k.$$

  where $\mathbf{x}_i(\Delta) = (x_1, \dots, x_i \pm \Delta, \dots, x_k)'$ and $\mathbf{x}$'s are chosen randomly from an L-level regular grid: $\{0, 1/(L-1), \dots, 1\}^k$.

- To understand the global effects of factors,

$$\mu_i = \frac{1}{l}\sum_{j=1}^{l} d_{i(j)} \quad \text{and} \quad \sigma_i = \sqrt{\frac{1}{l-1}\sum_{j=1}^{l}(d_{i(j)} - \mu_i)^2}.$$

- Campolongo (2007) proposed to use:

$$\mu_i^* = \frac{1}{l}\sum_{j=1}^{l} |d_{i(j)}|.$$

Morris design (1991) can be viewed as a collection of OFAT.

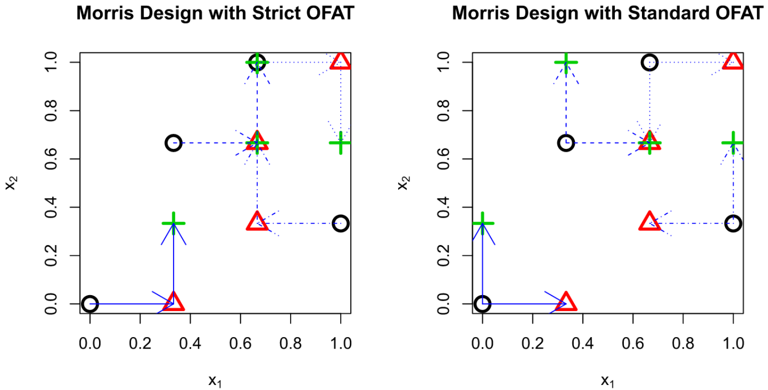

Figure: Morris design with strict OFAT (left) and standard OFAT (right). The OFAT structure is shown using arrows.

Sobol Methods (variance-based sensitivity analysis)

- ANOVA for square integrable functions:

$$\mathrm{var}(y) = V = \sum_{i=1}^{k} V_i + \sum_{i<j} V_{ij} + \cdots + V_{12\ldots k},$$

  where the variance components are $V_i = \mathrm{var}_{x_i}\{E_{x_{\sim i}}(y|x_i)\}$, $V_{ij} = \mathrm{var}_{x_i,x_j}\{E_{x_{\sim ij}}(y|x_i, x_j)\} - V_i - V_j$ and so on.
- The total Sobol' indices (Sobol, 2001; Saltelli et al., 2008) can be computed as

$$t_i = \frac{E_{x_{\sim i}}\{\mathrm{var}_{x_i}(y|x_{\sim i})\}}{\mathrm{var}(y)}, \quad i = 1, \ldots, k.$$

$$\text{Sob}(4,3) = \left[\underbrace{\begin{matrix} 0.500 & 0.500 & 0.500 \\ 0.250 & 0.750 & 0.250 \\ 0.750 & 0.250 & 0.750 \\ 0.125 & 0.625 & 0.875 \end{matrix}}_{\mathbf{A}} \; \underbrace{\begin{matrix} 0.500 & 0.500 & 0.500 \\ 0.750 & 0.250 & 0.750 \\ 0.250 & 0.750 & 0.250 \\ 0.875 & 0.625 & 0.125 \end{matrix}}_{\mathbf{B}}\right]$$

$$\mathbf{A}_B^{(1)} = \begin{matrix} 0.500 & 0.500 & 0.500 \\ 0.750 & 0.750 & 0.250 \\ 0.250 & 0.250 & 0.750 \\ 0.875 & 0.625 & 0.875 \end{matrix}$$

$$\mathbf{A}_B^{(2)} = \begin{matrix} 0.500 & 0.500 & 0.500 \\ 0.250 & 0.250 & 0.250 \\ 0.750 & 0.750 & 0.750 \\ 0.125 & 0.625 & 0.875 \end{matrix}$$

$$\mathbf{A}_B^{(3)} = \begin{matrix} 0.500 & 0.500 & 0.500 \\ 0.250 & 0.750 & 0.750 \\ 0.750 & 0.250 & 0.250 \\ 0.125 & 0.625 & 0.125 \end{matrix}$$

$$\hat{V}_i^{\text{tot}} = E_{x_{\sim i}}\{\mathbf{var}_{x_i}(y|x_{\sim i})\} = \frac{1}{2l}\sum_{j=1}^{l}\left\{y(\mathbf{A}_j) - y(\mathbf{C}_j^{(i)})\right\}^2 .$$

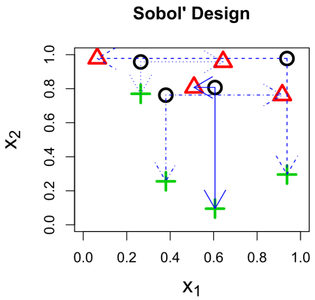

Morris design vs Sobol design

- Morris design can be written in the form of a Sobol' design when a standard OFAT is used.
- Sobol' can be converted to Morris if $\mathbf{A}_j \neq \mathbf{B}_j$.
- Morris is deterministic whereas Sobol' is random.

Outline

MOFAT

Define the maximum one-factor-at-a-time (MOFAT) design as the design $\mathbf{D}$ that maximizes $\sum_{j=1}^{l} |\mathbf{A}_{ji} - \mathbf{C}_{ji}^{(i)}|$ for all $i = 1, \ldots, k$, where $\mathbf{A}, \mathbf{C}^{(i)}$ $(i = 1, \ldots, k)$ are all LHDs.

Proposition

If the response surface is a realization of a Brownian motion field, then a MOFAT design maximizes the expected value of $\hat{V}_i^{tot}$ (i.e. Sobol' total index) for $i = 1, \ldots, k$.

Define a transformation function

$$T_l(x) = x - \lfloor l/2 \rfloor + l\mathbf{I}(x < (1 + l)/2).$$

Steps to construct MOFATs

- Starting from an $l \times k$ LHD $\mathbf{A}$, apply the transformation function T_l to all elements in $\mathbf{A}$ to form the matrix $\mathbf{B}$, i.e. $\mathbf{B}_{pq} = T_l(\mathbf{A}_{pq})$ for $p = 1, \ldots, l$ and $q = 1, \ldots, k$.
- For $i = 1, \ldots, k$, generate the matrix $\mathbf{C}^{(i)}$ via replacing the ith column of matrix $\mathbf{A}$ with the ith column of matrix $\mathbf{B}$.
- Aggregate matrices $\mathbf{A}, \mathbf{C}^{(1)}, \ldots, \mathbf{C}^{(k)}$ to get the n-run and k-factor design ($n = l(k+1)$):

$$\mathbf{D} = \begin{pmatrix} \mathbf{A} \\ \mathbf{C}^{(1)} \\ \vdots \\ \mathbf{C}^{(k)} \end{pmatrix}.$$

Proposition

For any l, designs generated by the foregoing three-step construction are MOFAT designs, where the minimum L_1-distance between any pair of $\mathbf{A}_{ji}$ and $\mathbf{B}_{ji}$ ($j = 1, \ldots, l$ and $i = 1, \ldots, k$) is $\lfloor l/2 \rfloor$ and the L_1-distance between the ith ($i = 1, \ldots, k$) column of matrices $\mathbf{A}$ and $\mathbf{C}^{(i)}$ is $\lfloor l^2/2 \rfloor$.

Proposition

MOFAT designs with at least three columns do not have duplicated rows.

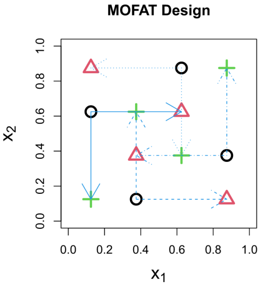

Figure: MOFAT design whose OFAT structure is shown using arrows.

Space-filling MOFATs

MOFAT can be further improved via selecting appropriate A towards space-filling property.

3-level MOFATs with $3(k+1)$ runs

In Step 1, the $3 \times k$ matrix $\mathbf{A}$ is generated via combining $\lfloor k/(3!) \rfloor$ replicates of $\mathbf{P}_3$ and the first $(k \pmod{3!})$ columns of $\mathbf{P}_3$ by columns.

$$\mathbf{P}_3 = \begin{pmatrix} 1 & 1 & 2 & 2 & 3 & 3 \\ 2 & 3 & 1 & 3 & 1 & 2 \\ 3 & 2 & 3 & 1 & 2 & 1 \end{pmatrix}.$$

Proposition

When using such a matrix $\mathbf{A}$ to construct MOFAT:

1. *$\mathbf{A}$ is the maximin L_1-distance design whose minimum L_1-distance is $\lceil 4k/3 \rceil$;*
2. *if $k > 3$, the resulting MOFAT design $\mathbf{D}$ has the minimum pairwise L_1-distance of 1 which appears $2k$ times, and it achieves the bound.*

An Example

$$\begin{pmatrix} 0.17 & 0.17 & 0.50 \\ 0.50 & 0.83 & 0.17 \\ 0.83 & 0.50 & 0.83 \\ \hline 0.83 & 0.17 & 0.50 \\ 0.17 & 0.83 & 0.17 \\ 0.50 & 0.50 & 0.83 \\ \hline 0.17 & 0.83 & 0.50 \\ 0.50 & 0.50 & 0.17 \\ 0.83 & 0.17 & 0.83 \\ \hline 0.17 & 0.17 & 0.17 \\ 0.50 & 0.83 & 0.83 \\ 0.83 & 0.50 & 0.50 \end{pmatrix}.$$

Outline

Naive implementation of sequential MOFAT

Consider a classic MOFAT with two sequential batches for an experiment with $k = 2$ factors.

First batch: $l_1 = 3$ levels, $l_1(k+1) = 9$ runs.

$$\mathbf{A}_1 = \begin{pmatrix} 0.17 & 0.17 \\ 0.50 & 0.83 \\ 0.83 & 0.50 \end{pmatrix}, \qquad \mathbf{B}_1 = \begin{pmatrix} \mathbf{0.83} & \mathbf{0.83} \\ \mathbf{0.17} & \mathbf{0.50} \\ \mathbf{0.50} & \mathbf{0.17} \end{pmatrix}$$

Second batch: $l_2 = 4$ levels, $l_2(k+1) = 12$ runs.

$$\mathbf{A}_2 = \begin{pmatrix} 0.125 & 0.125 \\ 0.375 & 0.375 \\ 0.625 & 0.875 \\ 0.875 & 0.625 \end{pmatrix}, \qquad \mathbf{B}_2 = \begin{pmatrix} \mathbf{0.625} & \mathbf{0.625} \\ \mathbf{0.875} & \mathbf{0.875} \\ \mathbf{0.125} & \mathbf{0.375} \\ \mathbf{0.375} & \mathbf{0.125} \end{pmatrix}$$

Observation: Juxtaposing $\mathbf{D}_1$ and $\mathbf{D}_2$ yields a design $\mathbf{D}$ with 21 runs, which is no longer MOFAT.

Interpolation-MOFAT

Transformation Function:

$$T_l'(x) = l + 1 - x, \quad \text{where } 1 \le x \le l \quad (1)$$

Construction Algorithm for I-MOFAT:

Algorithm 2 Construction of batch-sequential I-MOFAT design

Input: Set l levels and k factors.
Output: A batch-sequential I-MOFAT design $\boldsymbol{D}_I$.

1: Find an $l \times k$ LHD $\boldsymbol{A}_1$ and a $(l-1) \times k$ LHD $\boldsymbol{A}_2$, where the levels of $\boldsymbol{A}_1$ are coded as $1, 2, \ldots, l$, and the levels of $\boldsymbol{A}_2$ are coded as $1.5, 2.5, \ldots, l - 0.5$;
2: Let $\boldsymbol{A} = \begin{pmatrix} \boldsymbol{A}_1 \\ \boldsymbol{A}_2 \end{pmatrix}$, then apply the transformation function T_l' defined in (4) to all elements in $\boldsymbol{A} = [a_{pq}]$ to form the matrix $\boldsymbol{B} = [b_{pq}]$; that is, $b_{pq} = T_l'(a_{pq})$ for $p = 1, \ldots, l$ and $q = 1, \ldots, k$;
3: Follow Step 2 of Algorithm 1.
4: Follow Step 3 of Algorithm 1.

Theoretical Guarantee for I-MOFAT Design

Theorem

Let $\mathbf{A} = \begin{pmatrix} \mathbf{A}_1 \\ \mathbf{A}_2 \end{pmatrix}$, *where* $\mathbf{A}_1$ *is an* $l \times k$ *LHD with levels coded as* $1, 2, \ldots, l$, *and* $\mathbf{A}_2$ *is a* $(l-1) \times k$ *LHD with levels coded as* $1.5, 2.5, \ldots, l-0.5$. *Then the design*

$$\mathbf{D}_I = \begin{pmatrix} \mathbf{D}_1 \\ \mathbf{D}_2 \end{pmatrix}$$

obtained by the construction procedure is a MOFAT design.

When more than two batches are needed, extend $\mathbf{A}$ with additional matrices $\mathbf{A}_3, \mathbf{A}_4, \ldots$ constructed analogously to $\mathbf{A}_1$, i.e.,

$$\mathbf{A}^\top = \begin{pmatrix} \mathbf{A}_1^\top & \mathbf{A}_2^\top & \mathbf{A}_3^\top & \ldots \end{pmatrix},$$

then apply $T_l'(x)$ elementwise to obtain $\mathbf{B}$ and follow Steps 3–4.

Remarks for I-MOFAT

In particular, for the above Theorem to hold, the number of levels in $\mathbf{A}_1$ need not be $l - 1$, nor must the level coding use midpoints (e.g., $1.5, \ldots, l - 0.5$).

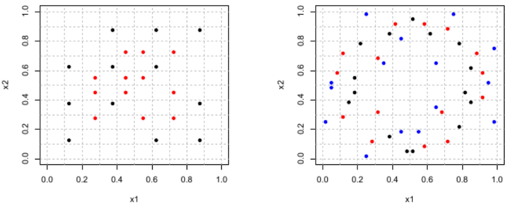

(a) (b)

Figure: (a) Batch-sequential I-MOFAT design with $k = 2$ and $l = 4$; (b) Batch-sequential S-MOFAT design with $t = 3$, $k = 2$, and $l = 15$.

Sliced-MOFAT

We develop another novel batch-sequential MOFAT design, the *S-MOFAT design*, inspired by the idea of *Sliced Latin Hypercube Designs (SLHD)*(Qian 2012).

Example

For $k = 2$ factors and $t = 3$ slices, consider a 9-run SLHD $\mathbf{X}$. For each slice $c = 1, 2, 3$, applying $\lceil \mathbf{X}_c / 3 \rceil$ produces a smaller LHD with 3 levels.

$$\mathbf{X}^\top = \begin{pmatrix} 1 & 7 & 4 & 6 & 2 & 8 & 3 & 9 & 5 \\ 3 & 5 & 9 & 2 & 6 & 8 & 1 & 4 & 7 \end{pmatrix} \quad (1)$$

Construction of S-MOFAT Design

Algorithm 3 Construction of batch-sequential S-MOFAT design

Input: Set t slices, l levels and k factors.
Output: A sequential S-MOFAT design $\boldsymbol{D}_S$.
1: Find an $l \times k$ SLHD $\boldsymbol{A}^{\mathrm{T}} = \left(\boldsymbol{A}_1^{\mathrm{T}} \vdots \cdots \vdots \boldsymbol{A}_t^{\mathrm{T}} \right)$, where the levels of $\boldsymbol{A}$ are coded as $1, 2, \ldots, l$;
2: Apply the transformation function $T_l^{'}$ defined in (4) to all elements $\boldsymbol{A} = [a_{pq}]$ to form the matrix $\boldsymbol{B} = [b_{pq}]$; that is, $b_{pq} = T_l^{'}(a_{pq})$ for $p = 1, \ldots, l$ and $q = 1, \ldots, k$;
3: Follow Step 2 of Algorithm 1;
4: Follow Step 3 of Algorithm 1.

Theorem: Validity of S-MOFAT Design

Theorem

Let $\mathbf{A}^\top = (\; \mathbf{A}_1^\top \quad \ldots \quad \mathbf{A}_t^\top \;)$, where $\mathbf{A}$ is an t-slice $l \times k$ SLHD with levels coded as $1, 2, \ldots, l$. Then the design $\mathbf{D}_S^\top = (\; \mathbf{D}_1^\top \quad \ldots \quad \mathbf{D}_t^\top \;)$ obtained by Algorithm is a MOFAT design.

Outline

Numerical Study: Modified Easom Function

We consider a modified Easom function (Pires et al., 2010; Xiao, Joseph, and Ray, 2023) with 10 input factors, $x_1, \ldots, x_{10} \in (-10, 10)$.

$$f(\mathbf{x}) = \cos(x_1)\cos(x_2)\Big[\exp\{-(x_1+c_1)^2-(x_2+c_2)^2\} - \exp\{-(x_1-c_1)^2-(x_2-c_2)^2\}\Big]$$

where the parameters c_1 and c_2 are independently drawn from $U(0, 10)$.

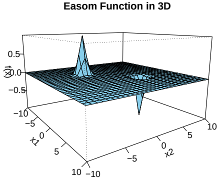

Screening Results: Modified Easom Function

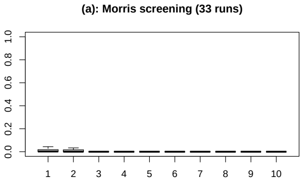

Figure: (a) Boxplots of $\sqrt{\mu_i}$ from the Morris screening method, and (b) Boxplots of $\sqrt{\hat{t}_i}$ from the Classic MOFAT design.

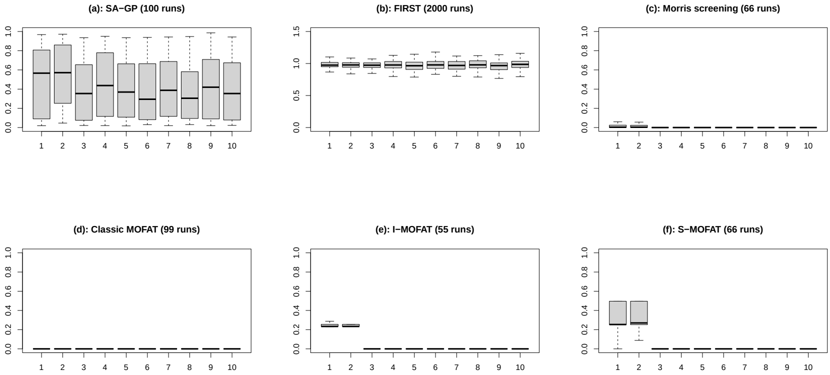

Figure: Boxplots of (a) $\sqrt{\hat{t}_i}$ from the SA-GP method, (b) $\sqrt{\hat{V}_i^{\text{tot}}}$ from FIRST, (c) $\sqrt{\mu_i}$ from Morris, (d) $\sqrt{\hat{t}_i}$ from Classic MOFAT, (e) $\sqrt{\hat{t}_i}$ from I-MOFAT, and (f) $\sqrt{\hat{t}_i}$ from S-MOFAT.

Numerical Study: Modified Borehole Function

We consider a modified eight-dimensional Borehole function (Worley, 1987), which models water flow through a borehole drilled from the ground surface through two aquifers.

$$f(\mathbf{x}) = \frac{2\pi T_u(H_u - H_l)}{\ln(r/r_w)\left(1 + \frac{2LT_u}{\ln(r/r_w)r_w^2K_w + \frac{T_u}{T_l}}\right)} \tag{2}$$

$$f(\mathbf{x}) = \begin{cases} \text{[Borehole function above]}, & a \leq r_w \leq b, \\ 0, & \text{otherwise}, \end{cases} \tag{3}$$

where $a = 0.07$ and $b = 0.13$. We added 12 inert factors $(x_9, \ldots, x_{20})$, following Moon (2012).

Screening Results: Modified Borehole Function

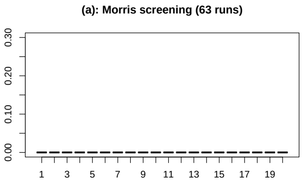

Figure: (a) Boxplots of $\sqrt{\mu_i}$ from Morris, and (b) Boxplots of $\sqrt{\hat{t}_i}$ from Classic MOFAT.

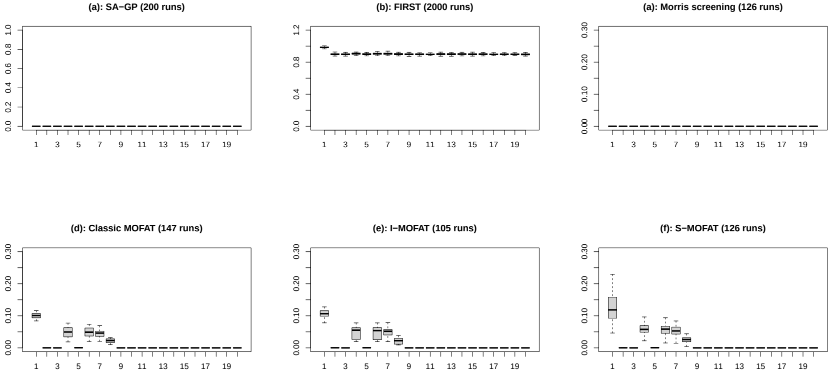

Figure: Boxplots of (a) $\sqrt{\hat{t}_i}$ from SA-GP, (b) $\sqrt{\hat{V}_i^{\text{tot}}}$ from FIRST, (c) $\sqrt{\mu_i}$ from Morris, (d) $\sqrt{\hat{t}_i}$ from Classic MOFAT, (e) $\sqrt{\hat{t}_i}$ from I-MOFAT, and (f) $\sqrt{\hat{t}_i}$ from S-MOFAT.

Outline

Case Study: Building Energy Analysis

We analyze building energy performance in China's severe cold climate zone using a typical multi-story office building baseline.

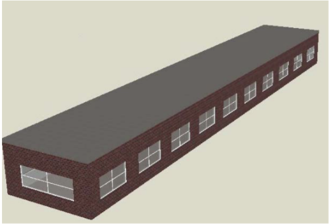

The baseline building follows GB 50189 standards: rectangular floor with 400 m^2 area and 3m height. We examine seven key design factors including Window-to-Wall Ratio, Insulation Thickness, Glazing U-value, Shading Coefficient, Building Orientation, HVAC Efficiency, and Outdoor Temperature, all assumed uniformly distributed.

5R1C Thermal Network Model

The 5R1C model represents building thermal dynamics using five thermal resistances and one capacitance, analogous to electrical circuits. Heat transfer flows through resistive elements while capacitance stores thermal energy.

$$\begin{aligned} R_1 \cdot (T_{sup} - T_i) + R_2 \cdot (T_s - T_i) + \Phi_i + f_{conv}\Phi_c &= 0 \\ R_5 \cdot (T_e - T_s) + R_2 \cdot (T_i - T_s) + R_3 \cdot (T_m - T_s) + \Phi_s + (1 - f_{conv})\Phi_c &= 0 \\ R_4 \cdot (T_e - T_m^\tau) + R_3 \cdot (T_s - T_m^\tau) + \Phi_m + \frac{C}{\Delta\tau}(T_m^{\tau-\Delta\tau} - T_m^\tau) &= 0 \end{aligned} \tag{4}$$

The model tracks thermal interactions among indoor air, surface, and thermal mass nodes. Internal gains and solar radiation are distributed as:

$$\Phi_i = \frac{1}{2}\Phi_{int}, \quad \Phi_s = \phi_s\left(\frac{1}{2}\Phi_{int} + \Phi_{sol}\right), \quad \Phi_m = \phi_m\left(\frac{1}{2}\Phi_{int} + \Phi_{sol}\right) \tag{5}$$

The model output is cooling load Φ_c, enabling accurate building energy performance evaluation.

Screening Results: Building Energy Model

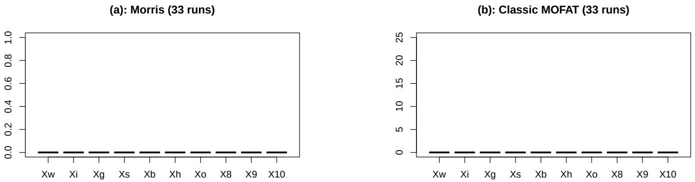

Figure: (a) Boxplots of $\sqrt{\mu_i}$ from the Morris design, and (b) Boxplots of $\sqrt{\hat{t}_i}$ from the Classic MOFAT method.

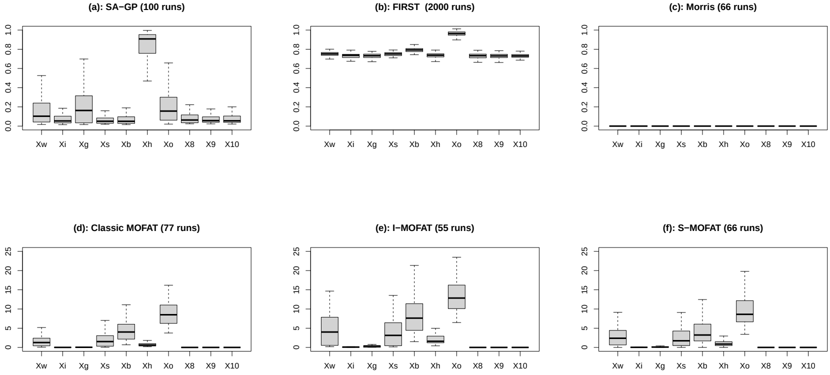

Figure: Boxplots of (a) $\sqrt{\hat{t}_i}$ from SA-GP, (b) $\sqrt{\hat{V}_i^{\text{tot}}}$ from FIRST, (c) $\sqrt{\mu_i}$ from Morris, (d) $\sqrt{\hat{t}_i}$ from Classic MOFAT, (e) $\sqrt{\hat{t}_i}$ from I-MOFAT, and (f) $\sqrt{\hat{t}_i}$ from S-MOFAT.

Case Study: satellite drag coefficients in low Earth orbit

Accurate estimation of satellite drag coefficients is critical for orbit prediction and collision avoidance in low Earth orbit (LEO). The U.S. Air Force Astrodynamics Standards *Committee* identifies atmospheric drag as the **largest source of orbital uncertainty**.

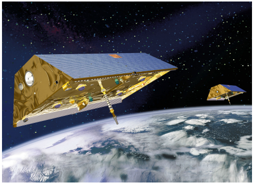

Figure: GRACE

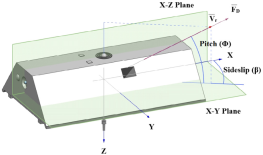

Figure: Mesh visual for GRACE satellite

The **Gravity Recovery and Climate Experiment (GRACE)** mission employs a Test Particle Monte Carlo (TPMC) model based on the Cercignani-Lampis-Lord (CLL) gas-surface interaction formulation. Each TPMC run requires about **3.3 minutes on a single core**. Exploring the full seven-dimensional input space–velocity, surface and atmospheric temperature, attitude angles, and two accommodation coefficients–would demand **18 million runs** (≈70,000 core hours).

Table: Free parameters in the drag simulator, together with their ASCII representations, physical meanings, units, and ranges. AC stands for accommodation coefficient.

Symbol	ASCII	Parameter	Units	Range
v_{rel}	`Umag`	velocity	m/s	$[5500, 9500]$
T_s	`Ts`	surface temperature	K	$[100, 500]$
T_a	`Ta`	atmospheric temperature	K	$[200, 2000]$
θ	`theta`	yaw	radians	$[-\pi, \pi]$
ϕ	`phi`	pitch	radians	$[-\pi/2, \pi/2]$
α_n	`alphan`	normal energy AC	unitless	$[0, 1]$
σ_t	`sigmat`	tangential momentum AC	unitless	$[0, 1]$

Screening results

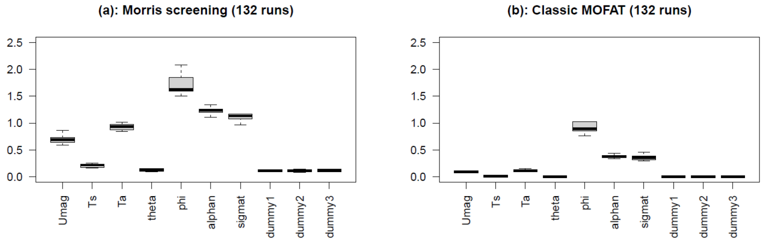

Figure: (a) Boxplots of $\sqrt{\mu_i}$ from the Morris design, and (b) boxplots of $\sqrt{\hat{t}_i}$ from Classical MOFAT.

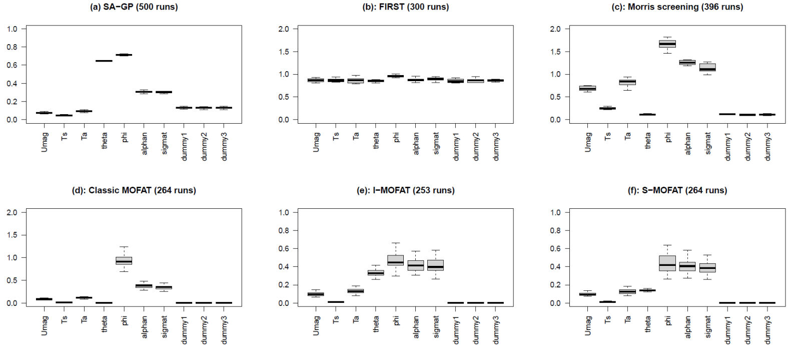

Figure: Boxplots of (a) $\sqrt{\hat{t}_i}$ from SA-GP, (b) $\sqrt{\hat{V}_i^{\text{tot}}}$ from FIRST, (c) $\sqrt{\mu_i}$ from Morris, (d) $\sqrt{\hat{t}_i}$ from Classical MOFAT, (e) $\sqrt{\hat{t}_i}$ from I-MOFAT, and (f) $\sqrt{\hat{t}_i}$ from S-MOFAT.

Using the same 5×10^5-training set, we compare the reduced six-variable laGP emulator with the original seven-variable emulator (including `Ts`).

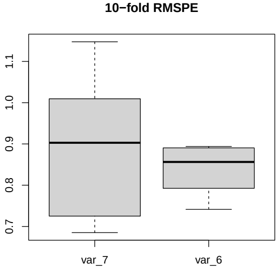

$$\text{RMSPE} = \sqrt{\frac{1}{n}\sum_{i=1}^{n}\left(\frac{\hat{Y}_i - Y_i}{Y_i}\right)^2} \times 100\%.$$

Figure: Cross-validation RMSPEs for laGP emulators built with all seven original physical variables and with the six screened variables.

Outline

Discussion and Future Directions

Key Challenges of Classic MOFAT:

- Unknown response surfaces make run size determination difficult
- Peak energy demand creates complex behavior requiring larger designs
- Rigid structure prevents sequential implementation
- Fails to reliably identify factors under limited data

Our Solution:

- I-MOFAT: Adaptive refinement with flexible batch sizing
- S-MOFAT: Systematic coverage with fixed batch expansion
- Both retain MOFAT's theoretical properties while enabling sequential deployment
- Superior performance in simulations and real-world applications

THANK YOU!!!